JOURNAL OF BACTERIOLOGY, Oct. 2009, p. 5921–5929 Vol. 191, No. 19
0021-9193/09/$08.00+0 doi:10.1128/JB.00642-09

Role of the Twin-Arginine Translocation Pathway in *Staphylococcus*▽†

Lalitha Biswas,[1] Raja Biswas,[1] Christiane Nerz,[1] Knut Ohlsen,[2] Martin Schlag,[1] Tina Schäfer,[2] Tobias Lamkemeyer,[3] Anne-Kathrin Ziebandt,[1] Klaus Hantke,[1] Ralf Rosenstein,[1] and Friedrich Götz[1]*

Institute of Microbial Genetics, University of Tübingen, Tübingen, Germany[1]; Institute for Molecular Infection Biology, University of Würzburg, Würzburg, Germany[2]; and Interfakultäres Institut für Zellbiologie, Proteome Centrum Tübingen, University of Tübingen, Tübingen, Germany[3]

Received 15 May 2009/Accepted 14 July 2009

In *Staphylococcus*, the twin-arginine translocation (Tat) pathway is present only in some species and is composed of TatA and TatC. The *tatAC* operon is associated with the *fepABC* operon, which encodes homologs to an iron-binding lipoprotein, an iron-dependent peroxidase (FepB), and a high-affinity iron permease. The FepB protein has a typical twin-arginine (RR) signal peptide. The *tat* and *fep* operons constitute an entity that is not present in all staphylococcal species. Our analysis was focused on *Staphylococcus aureus* and *S. carnosus* strains. Tat deletion mutants (Δ*tatAC*) were unable to export active FepB, indicating that this enzyme is a Tat substrate. When the RR signal sequence from FepB was fused to prolipase and protein A, their export became Tat dependent. Since no other protein with a Tat signal could be detected, the *fepABC-tatAC* genes comprise not only a genetic but also a functional unit. We demonstrated that FepABC drives iron import, and in a mouse kidney abscess model, the bacterial loads of Δ*tatAC* and Δ*tat-fep* mutants were decreased. For the first time, we show that the Tat pathway in *S. aureus* is functional and serves to translocate the iron-dependent peroxidase FepB.

The Sec pathway is the major secretion system that exports the majority of extracytosolic proteins in pro- and eukaryotes. Proteins are translocated through this pathway in a more or less unfolded state. A second protein export pathway was identified first in the chloroplast thylakoid membrane (8) and later in several bacteria (4, 14, 35). This pathway has been designated the twin-arginine translocation system (Tat), as the preproteins targeted to this pathway carry a characteristic amino acid motif, including two consecutive arginine residues, which are essential for the recognition by the Tat translocon. The Tat pathway operates independently of the Sec pathway and exports exoproteins across the bacterial cytoplasmic membrane, apparently in a fully folded conformation (3). Many of these proteins are complexed with cofactors.

Studies of several bacterial species, including *Escherichia coli* (37), *Bacillus subtilis* (22, 23), *Pseudomonas aeruginosa* (31), *Legionella pneumophila* (10, 11), and *Mycobacterium smegmatis* (29), have demonstrated that they possess a functional Tat export pathway. In *E. coli*, the TatA, TatB, and TatC proteins have been demonstrated to be essential for Tat-dependent protein translocation (4). However, several bacterial and archaeal species lack a TatB-like protein. For example, the *B. subtilis* genome encodes three TatA- and two TatC-like proteins. Thus, at least one copy of the TatA homologue and one copy of the TatC homologue are required for a functional Tat pathway. In *Bacillus subtilis*, several proteins were predicted that could potentially use the Tat pathway, as their signal peptides (SPs) contain RR or KR motifs. However, proteomic analysis revealed that 13 proteins with potential RR/KR SPs were Tat independent, showing that the Tat machinery does not recognize their RR/KR motifs. In fact, only the phosphodiesterase PhoD and the newly identified YwbN protein were shown to be secreted in a strictly Tat-dependent manner (22). YwbN is part of the YwbLMN operon product and is involved in the uptake of free ferric iron (32).

For staphylococci, very little information regarding the function of the Tat system exists. A *tatC*-deficient mutant showed little difference from the wild type (WT) in its extracellular protein pattern (48). In another study, green fluorescent protein (GFP) was fused with the SP of the *E. coli* TorA protein and the subcellular localization of the hybrid protein was compared in *Staphylococcus carnosus* and its *tatC* mutant (30). The results showed that GFP was secreted in neither the WT nor the *tatC* mutant but was stuck in the cell wall fraction of the WT. However, no Tat-transported protein has been identified in staphylococci so far.

Here we show that the *tat* operon encoding TatA and TatC is present in *Staphylococcus aureus*, *S. carnosus*, and *Staphylococcus haemolyticus* but is missing in a number of other staphylococcal species. By comparative analysis of WT and *tatAC* mutant strains, the functionality of the Tat pathway in *S. carnosus* and *S. aureus* was demonstrated, and it was found that the iron-dependent peroxidase (FepB) is translocated by the Tat system. The Tat system can efficiently translocate heterologous proteins such as lipase or protein A when it is fused with the SP of FepB. ^{55}Fe transport experiments demonstrated that FepABC is involved in iron uptake.

MATERIALS AND METHODS

Identification of Tat substrates by ParSeq, a modified TATFIND algorithm. The Tat SP of peroxidase was identified in staphylococcal genomes by use of the software tool ParSeq, a program that combines the search for motifs with a

* Corresponding author. Mailing address: Mikrobielle Genetik, Universität Tübingen, Auf der Morgenstelle 28, D-72076 Tübingen, Germany. Phone: (49) 7071 29746-36. Fax: (49) 7071 295039. E-mail: friedrich.goetz@uni-tuebingen.de.

† Supplemental material for this article may be found at http://jb.asm.org/.

▽ Published ahead of print on 24 July 2009.

TABLE 1. Bacterial strains used in this study[a]

Species and strain	Relevant characteristic(s)	Source or reference
S. aureus		
SA113 (ATCC 35556)	Derivative of RN1 (NCTC8325), *agr*, 11-bp deletion in *rbsU*	21
RN4220	NCTC8325 derivative	21
RN1HG	Derivative of RN1 (NCTC8325), with *rsbU* repaired	Herbert et al., unpublished data
SA113 (Δ*tatAC*)	*tatAC*::*ermC*	This study
SA113 (Δ*tat-fep*)	*tat-fep*::*kan*	This study
S. carnosus		
TM300	WT	38
Δ*tatAC*	*tatAC*::*ermC*	This study
S. epidermidis ATCC 14990	WT	17
S. haemolyticus CCM2737	WT	17
S. simulans ATCC 27848	WT	24
S. saprophyticus DSM20229	WT	39
S. lugdunensis ATCC 43809	WT	15
S. gallinarum Tu 3928	WT	13
S. muscae DSM 7068	WT	20
S. sciuri subsp. *lentus* DSM 20352	WT	
S. capitis subsp. *capitis* CCM 2734	WT	24
S. hyicus subsp. *hyicus* NCTC10350	WT	12

[a] For more detailed information regarding the species characteristics, see reference 16.

search for certain structural properties (40). The search pattern used was $X_1RRX_2X_3X_4$, in which the amino acid at position X_1 had a hydrophobicity score of <0.26, X_2 had to be one of certain residues (ARKDEF), X_3 had a hydrophobicity score of >0.77 (positively charged residues were excluded from this position), and X_4 was one of certain residues (ILVMF). All hydrophobicity values were described previously (9). In addition, the following three criteria were considered: (i) whether there was an uncharged stretch of at least 13 residues in the 22 residues following the RR; (ii) whether the hydrophobicity value of the first 13 residues of the uncharged region was <8.0; and (iii) since it is known that SPs should be in the beginning of an open reading frame, the twin-arginine motif was expected to be within the first 30 amino acids. All of these constraints were used to construct a search pattern in the form of a regular expression in ParSeq. With this regular expression, we searched the whole genomes of *S. aureus* and *S. carnosus*. If the search identified a sequence that matched the above pattern, the corresponding gene was considered to possess a putative Tat signal sequence.

Bacterial strains. Bacterial strains used in this study are listed in Table 1.

Construction of *tatAC* deletion mutants in *S. carnosus* and *S. aureus*. The upstream flanking regions of *tatA* were amplified using the primer pair SCtat up F (5′-TAACATGAATTCCATTGATATTCATTTC-3′; EcoRI site is underlined) and SCtat up R (5′-TACATTGGTACCAAGTTGATCCAATAG-3′; KpnI site is underlined) for *S. carnosus* TM300 and the primer pair SAtatC up F (5′-TAACATGAATTCTAATTACACTGTAAATG-3′; EcoRI site is underlined) and SAtatC up R (5′-TACATTGGATCCTAAAATTTTTACTAACCG-3′; BamHI site is underlined) for *S. aureus* SA113. To amplify the downstream flanking regions of *tatC*, the primer pairs SCtat down F (5′-TAACATCTGCAGAACAAACACCCGTC-3′; PstI site is underlined) and SCtat down R (5′-TACATTGCTAGCTTCAGATTTGGC-3′; NheI site is underlined) for *S. carnosus* TM300 and SAtatC downF (5′-TAACATCTGCAGCCTTATACGAATCAATGC-3′; PstI site is underlined) and SAtatC downR (5′-TACATTGATATCAAATTCAAACTAAAGACGG-3′; EcoRV site is underlined) for *S. aureus* SA113 were used for PCR amplification and cloning into the multiple cloning site of pBT2 (7). The *ermB* cassette from pEC2 was introduced between the flanking regions. *S. carnosus* Δ*tatAC* and *S. aureus* Δ*tatAC* mutants were constructed by a standard homologous recombination method (7). The *tatAC* deletion mutants were identified by their erythromycin-resistant and chloramphenicol-sensitive phenotype and were confirmed by PCR and DNA sequence analyses.

Construction of *tat-fep* deletion mutant in *S. aureus*. A 1-kb fragment resembling the upstream region of *tatA* and a 1-kb fragment identical to the region upstream of SA0331 were amplified by PCR, using the primers SA ptupF (5′-TATTATGGATCCAAAATTCCACCTATGATACC-3′; BamHI site is underlined), SA ptupR (5′-TAACATCCATGGCCTCACTCATAAGTAG-3′; NcoI site is underlined), Sa ptdwnF (5′-TAACATAGATCTTTTGACACCTCATTATAGAAATTC-3′; BglII site is underlined), and Sa ptdwnR SmaR (5′-TATTATCCCGGGTGGGTCCGTAATTTC-3′; SmaI site is underlined). The resulting PCR products were cloned into the multiple cloning site of pDG782 (19). The Δ*tat-fep*::*kan* fragment, representing the upstream fragment, the *aphAIII* cassette, and the downstream fragment, was moved into the plasmid pKOR1 (1) by using Gateway technology (Invitrogen), resulting in plasmid pKOR1-Δtat-fep::kan. Allelic replacement in *S. aureus* was performed as described previously (1). The Δ*tat-fep* deletion mutants were identified by their kanamycin-resistant and chloramphenicol-sensitive phenotype and were confirmed by PCR and DNA sequence analyses.

Construction of vectors containing Tat SP fused to lipase and protein A. Protein A and prolipase were used as reporter enzymes. Prolipase was originally derived from *Staphylococcus hyicus* (18, 26). The prolipase (*pro-lip*) and protein A (*spa*) genes were fused with the Tat SP sequence of the *S. carnosus*-specific iron-dependent peroxidase gene (SC2214). The DNA fragments were inserted in pCX19 in such a way that expression of the target gene was under the control of the xylose-inducible promoter (5, 47). The DNA fragment encoding the peroxidase Tat SP was amplified from *S. carnosus* chromosomal DNA by use of the primer pair 5′-TACATTGGATCCTAGGAGGTGACGATATGACACAAGACAAGC-3′ (BamHI site is underlined) and 5′-TATCATTCTAGAGAAAGAAAAAATGCCGCCGACTCC-3′ (XbaI site is underlined). The prolipase gene was amplified from pTX15 by PCR (33), using the primers 5′-TACATTTCTAGAAATGATTCGACAACACAAAC-3′ (XbaI site is underlined) and 5′-TATCATGAGCTCTCATTATGCGTTCTTTGTGCTTTC-3′ (SacI site is underlined). The prolipase gene was ligated with the signal sequence of the peroxidase gene and cloned into pDG782 (19). The gene fusion was subsequently recloned into the staphylococcal vector pCX19, using BamHI and PstI, resulting in pCXRR-lip; the corresponding gene was under the control of the xylose-inducible promoter. The vector pCX19 encodes prolipase fused to the Sec SP. The protein A (*spa*) gene was fused to the Tat signal sequence by amplifying *spa* from the *S. aureus* DNA template by PCR using the following primers: TACATTGTCGACGCGCAACACGATGAAGC (SalI site is underlined) and TAACATCCCGGGTTATAGTTCGCGACG (SmaI site is underlined). The PCR fragment was digested and ligated into pCXRR-lip precut with the same restriction enzymes, replacing the *lip* gene. The resulting plasmid was designated pCXRR-spa.

Lipase and peroxidase activity assays. Staphylococcal cultures were induced with 0.5% xylose and grown until late stationary phase. Cells were pelleted by centrifugation at 13,000 × *g* for 5 min, and the culture supernatant was filtered through 0.22-μm-pore-size filters and used for the detection of secreted lipase, peroxidase, and protein A.

Lipase activity was measured spectrophotometrically at 405 nm, using *p*-nitrophenyl-caprylate as a substrate (45, 47), in stationary-phase culture supernatants as well as in the zymogram gel (26). Briefly, after sodium dodecyl sulfate-polyacrylamide gel electrophoresis analysis, the gels were washed once in 20% isopropanol for 2 min, followed by three washes with 50 mM Tris-HCl (pH 7.5) for 5 min. Finally, the gels were laid on lipase test medium (0.1% agarose, 1 mM $CaCl_2$, 50 mM Tris-HCl, 1% Tween 20, pH 7.5) and incubated at 37°C until halo bands were visible.

To detect the amount of secreted peroxidase, an Amplex red hydrogen per-

oxide/peroxidase assay kit (Molecular Probes, Eugene, OR) was used according to the manufacturer's instructions. This assay was performed spectrophotometrically. Absorbance was measured at 560 nm by using a microtiter plate reader (SpectraMAX UV-visible spectrophotometer).

Isolation of anchored and cytoplasmic protein A. To detect protein A, stationary-phase staphylococcal cultures (50 ml) were pelleted by centrifugation at 13,000 × *g* for 15 min, and the supernatant was removed (secreted fraction). The cell pellet was resuspended in 5 ml of TRN buffer (50 mM Tris-HCl [pH 7.5], 30% raffinose, 145 mM NaCl) containing 0.1 mg/ml lysostaphin and incubated at 37°C for 30 min. Raffinose was added to prevent cell lysis by lysostaphin treatment. The sample was centrifuged, and the supernatant was removed (cell wall-associated fractions). To obtain cytoplasmic fractions, the cell pellet was resuspended in lysis buffer (50 mM Tris-HCl [pH 7.5], 145 mM sodium chloride, 0.1 mg of lysostaphin per ml) and subjected to lysis at 37°C for 30 min, followed by centrifugation of the lysate for 30 min at 100,000 × *g*, and the supernatant was collected (cytoplasmic fraction). Subsequently, an aliquot of each fraction was subjected to sodium dodecyl sulfate-polyacrylamide gel electrophoresis, followed by immunoblotting analysis using a protein A-specific antibody (Gene Tex, Inc.).

Immunofluorescence microscopy. To detect cell wall-anchored protein A by immunofluorescence microscopy, *S. carnosu*s and its Δ*tatAC* deletion mutant harboring the plasmid pCXRR-spa were grown in Trypticase soy broth to mid-log phase, and the culture was centrifuged and washed twice in phosphate-buffered saline (PBS) before incubation (60 min at room temperature) with an Alexa Fluor 594-conjugated anti-rabbit secondary antibody. Following two washes in PBS, the cells were resuspended in 1 ml PBS to an optical density at 600 nm (OD_{600}) of 1, and slides were prepared.

Analysis of exoproteins by 2D gel electrophoresis. *S. aureus* and *S. carnosus* parent strains and their respective *tatAC* mutant strains were cultured for 12 h and 24 h at 37°C. Cells were pelleted by centrifugation, and the culture supernatants were filtered through 0.22-μm-pore-size filters. Exoproteins were isolated and analyzed by two-dimensional (2D) gel electrophoresis as described earlier (34).

Identification of *tatAC* genes in *Staphylococcus*. The genomic DNAs of 12 different staphylococcal species, *S. aureus*, *S. carnosus*, *Staphylococcus epidermidis*, *S. haemolyticus*, *Staphylococcus saprophyticus*, *Staphylococcus simulans*, *Staphylococcus lugdunensis*, *Staphylococcus gallinarum*, *Staphylococcus muscae*, *Staphylococcus lentus*, *Staphylococcus capitis*, and *S. hyicus*, were used as templates for the identification of the putative *tatA* and *tatC* genes, using the primer pair tatAF (5′-GCTTTAATTA TTTTTGGTCC-3′) and tatCR (5′-CAGGTGCAATGAATGCCCACAATTG-3′). As described elsewhere (2), broad-range primers SSU-bact-27f (5′-AGAGTTTGA TCMTGGCTCAG-3′) and SSU-bact-907r (5′-CCGTCAATTCMTTTRAGTTT-3′) were used to amplify the 16S rRNA gene as a PCR control.

Iron transport assay. For iron uptake experiments, cells were grown in Chelex-treated M9 minimal medium supplemented with 1% Casamino Acids and 5% minimum essential medium-vitamin solution. The medium was made iron deficient by being supplemented with 200 μM 2,2′-dipyriyl. Cells were harvested when the cultures reached an OD_{578} of 0.8 to 1 and were washed twice with M9 transport medium (Chelex 100-treated 1× M9 salts, 1 ml of 1 mM $MgSO_4$, 0.1% glucose) at 4°C. Cells were resuspended in M9 transport medium (Chelex 100-treated 1× M9 salts, 100 mM morpholineethanesulfonic acid, pH 6, 1 ml of 1 mM $MgSO_4$, 0.1% glucose) to an OD_{578} of 1.0 and kept on ice; the cells were incubated with shaking at 37°C for 5 min before the onset of transport. ^{55}Fe reduced with ascorbate (100 μM [5.5 kBq/ml]/100 mM ascorbate) was diluted 100-fold in the cell suspension. Samples (0.7 ml) were taken at the indicated times, filtered on mixed-cellulose GN-6 Metricel membrane filters (Pall), washed twice with 2 ml 0.1 M LiCl solution, dried, and counted with a liquid scintillation counter after addition of a scintillator.

Mouse infection studies. Female BALB/c mice (16 to 18 g) were purchased from Charles River, Sulzfeld, Germany, housed in polypropylene cages, and received food and water ad libitum.

S. aureus strains were cultured for 18 h in B medium, washed three times with sterile 0.9% NaCl, and suspended in sterile 0.9% NaCl to 7.0×10^7 CFU/100 μl. As a control, selected dilutions were plated on B agar. Mice were inoculated with 100 μl of *S. aureus* via the tail vein. Control mice were treated with sterile NaCl. For each strain, seven mice were used. Five days after challenge, the animals were sacrificed and kidneys were aseptically harvested and homogenized in 3 ml of 0.9% NaCl, using Dispomix (Bio-Budget Technologies GmbH, Krefeld, Germany). Serial dilutions of the organ homogenates were cultured on mannitol salt-phenol red agar plates for at least 48 h at 37°C. CFU were calculated as CFU/gram of kidney. The statistical significance of bacterial load differences was determined using the Mann-Whitney test.

RESULTS

Presence of the Tat system in *Staphylococcus* species. A genome-wide search of *S. carnosus* for the Tat SP revealed that the iron-dependent peroxidase FepB (Sca2214) contains a typical Tat signal sequence composed of the core sequence SRRFFLK followed by a weakly hydrophobic domain and a possible cleavage site (IGA). FepB revealed 40% similarity to YwbN of *Bacillus subtilis*, and among the staphylococcal species, it showed 71 to 75% sequence identity. As opposed to the published sequence annotation (25, 46), it turned out that the translational start sites of FepB in the *S. aureus* N315 (SA0332) and *S. haemolyticus* (SH0685) sequences begin 38 and 27 codons upstream, respectively (see Fig. 2A). This explains why the Tat SP was apparently not recognized in the corresponding reports. The FepB homologues of other bacterial species from different phyla also have typical Tat signal sequences (Table 2).

In the genome of *S. aureus*, *tatA* (SA0335) and *tatC* (SA0334), encoding the Tat secretion system, are organized in an operon. Another operon, encoding a lipoprotein (SA0331), an iron-dependent peroxidase (SA0332), and a high-affinity iron transporter (SA0333), is found downstream of *tatC*. It has been designated the *fepABC* operon. A region of dyad symmetry resembling a ferric uptake regulatory binding site (Fur box) precedes the lipoprotein gene (*fepA*). Two REGXE motifs, which have been implicated in iron binding (42), are found in the high-affinity iron transporter protein, at positions 331 to 335 and 449 to 453. The organization of this *tat* and *fep* operon cluster is conserved in the genomes of *S. aureus*, *S. carnosus*, and *S. haemolyticus* (Fig. 1A). Homologs of the *fep* operon are found in several bacteria, including *Escherichia coli*, *Bacillus subtilis*, *Streptomyces coelicolor*, *Streptococcus thermophilus*, *Pseudomonas syringae*, *Neisseria meningitidis*, *Yersinia pestis*, and *Klebsiella pneumoniae*.

Tat deletion mutants of *S. carnosus* and *S. aureus*. To examine the functionality of the Tat pathway in *Staphylococcus* species, deletion mutants were created in *S. carnosus* TM300 and *S. aureus* SA113 by replacing both the *tatA* and *tatC* genes with an erythromycin resistance cassette (*ermB*) (7) (Fig. 1B). The *S. aureus* Δ*tat-fep* operon was created by replacing the *tatAC* and *fep* operons with a kanamycin (*kan*) resistance cassette (Fig. 1C). The Δ*tatAC* mutants were complemented with the plasmid pTX-tat, which was constructed by cloning the *tat* genes under the control of a xylose-inducible promoter (Fig. 1D). The mutant strains from both species are similar to their respective WT strains in terms of growth rate and colony morphology in tryptic soy broth and B medium (data not shown).

FepB, an iron-dependent peroxidase, is a Tat substrate. To test whether the iron-dependent peroxidase FepB, with a predicted Tat signal sequence, is secreted in a Tat-dependent manner, we examined the presence of peroxidase activity in the culture supernatants of *S. carnosus* WT, its Δ*tatAC* deletion mutant, and its complemented mutant, *S. carnosus* Δ*tat* (pTX-tat). Peroxidase activity was found only in the culture supernatants of *S. carnosus* WT and its complemented mutant, not in the culture supernatants of the Δ*tatAC* mutant (Fig. 2B). Similar results were obtained with *S. aureus* WT and its Δ*tat*AC mutant.

***tat* mutants are unable to export lipase fused to the FepB SP.** In order to investigate the ability of the Tat system to

TABLE 2. SP sequences of FepB homologs in other bacteria

Species[a]	SP sequence
sau	MTNYEQVNDSTQFS**RR**TFLKMLGIGGAGVAIGA
eco	MQYKDENGVNEPS**RR**LLKVIGALALAGSCPVAHA
apl	MMAEIRS**RR**DFLKNTALVGAGLLSAPAFA
bma	MLVGAGRSGLTSRSARGAAPRA**RR**HRVGGRAPRWAEANATRRSRGACTRAVA
bsu	MTASNEEKWMNKKIS**RR**DMLKLTGIGVAGVAIGASGLGGLA
cgl	MVS**RR**GFLGGAGLIAGASALA
eta	MAKKTDEVASAS**RR**LLKGVGILSGALAVAGGCPAHA
kpn	MAQQKPHDVNEPS**RR**LLKGIGALGGALAITGGCPVAHA
lmo	MTDKKSENQTEKTETKENKGMT**RR**EMLKLSAVAGTGIAVG A
msm	MTPAQPSGIS**RR**KLFGAAGVTAAVVGAASAGALAGRASA
nmc	MSKKQPAQPT**RR**TLFKTAIAAGA
pst	MKTPDSNPDATNAPVSLQ**RR**RVLMGLGAAGAALAGSSLSGNVLAAA
sbo	MQYKDENGVNEPS**RR**LLKVIGALALAGSCPVAHA
sco	MTDTDSPAPAPSPS**RR**SLIGWGGAGLALGAAAAAGGAVA
sgo	MTNDEKWFEKKMD**RR**EFLKKAGIGGAGLALGVSGASA
ssa	MTNDEKWFNKKMD**RR**EFLKKAGIGGAGLALGVSGASA
ste	MTDKKFLDQKMD**RR**EFLKKSGIGGAGLALGLSGASA
ype	MRDKTGPKFGPYQPDDEAVSPS**RR**LILGMGMVSGALVLGGAKTAQA
yps	MRDKTGPKFGPYQPDDEAVSPS**RR**LILGMGMVSGALVLGGAKTAQA

[a] sau, *Staphylococcus aureus*; eco, *Escherichia coli*; bsu, *Bacillus subtilis*; ype, *Yersinia pestis*; sco, *Streptomyces coelicolor*; kpn, *Klebsiella pneumoniae*; msm, *Mycobacterium smegmatis*; lmo, *Listeria monocytogenes*; cgl, *Corynebacterium glutamicum*; yps, *Yersinia pseudotuberculosis*; eta, *Erwinia tasmaniensis*; sbo, *Shigella boydii*; sgo, *Streptococcus gordonii*; ssa, *Streptococcus sanguinis*; apl, *Actinobacillus pleuropneumoniae*; pst, *Pseudomonas syringae*; nmc, *Neisseria meningitidis*; ste, *Streptococcus thermophilus*; bma, *Burkholderia mallei*.

secrete heterologous proteins in *S. carnosus*, we fused the Tat SP of FepB to the prolipase (*pro-lip*) gene (Fig. 3A). The resulting plasmid, pCXRR-lip, was transformed into *S. carnosus* and *S. carnosus* Δ*tatAC*, and their culture supernatants were tested for lipase activity. In contrast to *S. carnosus* WT(pCXRR-lip), no lipase was detected in the culture supernatants of *S. carnosus* Δ*tatAC*(pCXRR-lip) (Fig. 3B). Analysis of the cytoplasmic fractions of the strains revealed the expression of lipase in both *S. carnosus* WT and the Δ*tatAC* mutant, suggesting that in the absence of the Tat transport pathway, lipase secretion is blocked and accumulates within the cells of the Δ*tatAC* mutant (Fig. 3C). This intracellular accumulation of lipase is very likely responsible for the slower growth (data not shown) of *S. carnosus* Δ*tatAC*(pCXRR-lip).

To confirm that the secretion deficiency of lipase in the *S. carnosus* Δ*tatAC* mutant was indeed specific for the Tat system, Sec-dependent lipase secretion was also analyzed in this mutant. The secretion efficiencies of the lipase via the Sec machinery in *S. carnosus* Δ*tatAC* and its parental *S. carnosus* strain carrying plasmid pCX19 were comparable, indicating that secretion of the lipase with its Sec SP is not affected in the Δ*tatAC* mutant (Fig. 3B and C).

The Tat secretion system allows the anchoring of protein A (Spa) to peptidoglycan. Protein A has a sorting sequence and

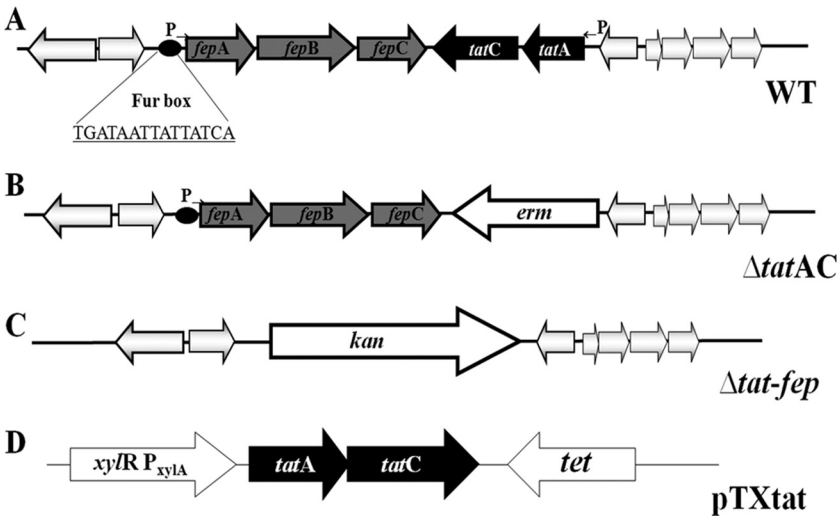

FIG. 1. (A) Gene organization of *fepABC* and *tat* operons of *Staphylococcus*. The *fepABC* operon encodes a lipoprotein, an iron-dependent peroxidase, and a high-affinity iron transporter. Arrows indicate the orientation of the genes, and the circle represents a putative Fur box. (B) Allelic replacement of *tatAC* operon by an erythromycin resistance cassette in *S. aureus* and *S. carnosus*. (C) Allelic replacement of *fepABC* and *tatAC* operons by a kanamycin resistance cassette in *S. aureus*. (D) Relevant part of plasmid pTX-*tat*, carrying *tatAC* genes under the control of a xylose-inducible promoter.

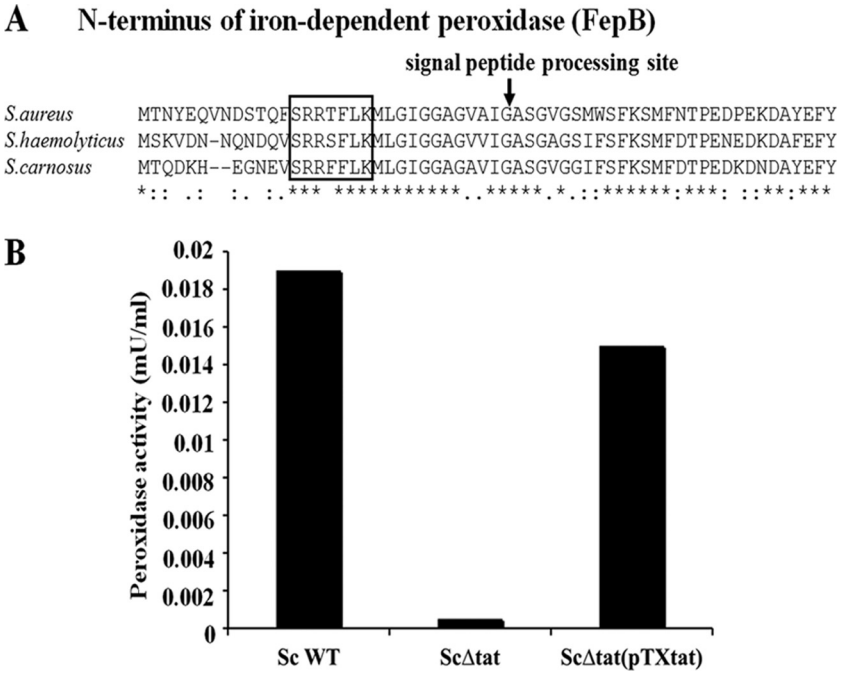

FIG. 2. The iron-dependent peroxidase FepB is a Tat substrate. (A) Multiple amino acid sequence alignment of the N terminus of FepB of *S. aureus*, *S. haemolyticus*, and *S. carnosus*, using Clustal W. Asterisks indicate identical amino acid residues. The twin-arginine motif in the sequence is boxed. The arrow indicates the processing site. (B) Culture supernatants of *S. carnosus* WT, the *S. carnosus* Δ*tat* mutant, and its complemented mutant, *S. carnosus* Δ*tat*(pTX-tat), were tested for the presence of peroxidase by use of an Amplex red peroxidase assay kit.

is covalently anchored to peptidoglycan (41). To find out whether the sortase can recognize a Tat-secreted protein and anchor it to the peptidoglycan, the Tat SP of FepB from *S. carnosus* was fused with the protein A (*spa*) gene and transformed via plasmid pCXRR-spa (Fig. 4A) into *S. carnosus* and *S. carnosus* Δ*tatAC*. Protein A expression was monitored by Western blotting. In the culture supernatant and cell wall-associated fractions, protein A was detected only in *S. carnosus*-(pCXRR-spa) and *S. aureus* (control). However, no protein A was detectable in *S. carnosus* Δ*tatAC*(pCXRR-spa) (Fig. 4B). Alexa Fluor 594-conjugated antibody labeling also revealed the anchoring of protein A only in *S. carnosus* WT(pCXRR-spa), not in *S. carnosus* Δ*tatAC*(pCXRR-spa) (Fig. 4C). In the cytoplasmic fraction, protein A was detected in both *S. carnosus* WT and its Δ*tatAC* mutant (Fig. 4B), indicating that although protein A is expressed in both strains, it can be neither secreted nor anchored in the Δ*tatAC* mutant.

Exoprotein pattern analysis by 2D gel electrophoresis. To identify proteins secreted via the Tat pathway, the exoproteins of the *S. aureus* and *S. carnosus* parent strains and their respective *tatAC* mutants were analyzed by 2D gel electrophoresis. However, no marked difference was observed between the parent strains and their Δ*tatAC* mutants. Although a clear difference in peroxidase activity between *S. carnosus* WT and its Δ*tatAC* mutant could be seen, we were unable to identify the peroxidase protein in 2D gels in all four independent assays (data not shown). This result is in accordance with a previous study (48).

Identification of *tatAC* genes in other staphylococci. Genome sequence analysis showed that the *tatAC* operon is present in *S. carnosus*, *S. aureus*, and *S. haemolyticus* and absent in *S. epidermidis* and *S. saprophyticus.* PCR analysis with various strains suggested that *tatAC* genes are also present in *S. gallinarum* and *S. lugdunensis* but are absent in quite a number of other staphylococcal species, including *S. capitis*, *S. hyicus*, *S. lentus*, *S. muscae*, and *S. simulans*, indicating that the Tat pathway is not a common secretory pathway in staphylococci. Our PCR results were corroborated by the genome sequence databases available for various staphylococcal species (including all sequenced strains of *S. aureus* and *S. epidermidis* and sequenced representatives of *S. carnosus*, *S. haemolyticus*, and *S. saprophyticus*).

Role of FepABC in iron transport. The ability of the *fepABC* operon to transport iron was investigated using ^{55}Fe uptake assays. *S. aureus*, *S. aureus* Δ*tatAC*, and *S. aureus* Δ*tat-fep* were grown under iron-sufficient and iron-depleted conditions. Although growth was decreased in iron-deficient medium, no difference in growth rate was observed among the strains (data not shown). Strains grown under iron-sufficient conditions displayed comparable iron uptake rates. A significant decrease in the ability to transport iron was observed in the Δ*tat-fep* mutant compared to the WT. The rate of iron uptake by the Δ*tatAC* mutant was also decreased compared to that of the WT, although to a lesser degree (Fig. 5A).

Comparative virulence in a mouse kidney abscess model. To assess the role of the *tat* and *fep* operons in virulence, the Δ*tatAC* and Δ*tat-fep* mutations were transduced into strain RN1HG, which is more virulent than strain SA113 (S. Herbert et al., unpublished data) and has functional global regulators, such as *agr*, *sigB*, and *sarA*. Virulence was investigated in a hematogenic kidney abscess model with *S. aureus* RN1HG WT, RN1HG Δ*tatAC*, and RN1HG Δ*tat-fep*. Mice were challenged with 7×10^7 CFU via the tail vein, and bacterial loads

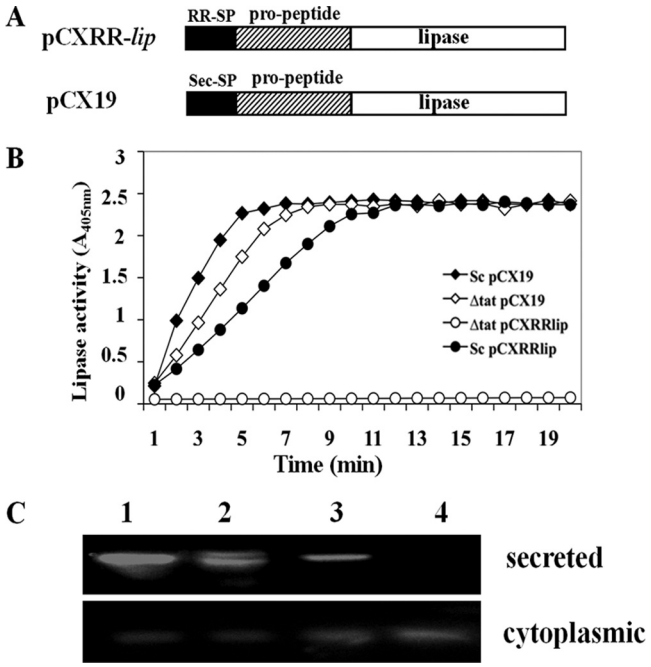

FIG. 3. Expression of lipase fused to RR-SP. (A) Illustration of the primary structures of lipase with the Tat SP and propeptide, as expressed with plasmid pCXRR-lip, and the lipase fused to the Sec SP and propeptide, as expressed with plasmid pCX19. (B) *p*-Nitrophenyl-caprylate-based lipase assay with culture supernatants of *S. carnosus*(pCX19) (◆), *S. carnosus* Δ*tatAC*(pCX19) (◇), *S. carnosus*(pCXRR-lip) (●), and *S. carnosus* Δ*tatAC*(pCXRR-lip) (○). (C) Lipase activity staining (zymogram) of culture supernatants and whole-cell extracts. Lane 1, *S. carnosus*(pCX19); lane 2, *S. carnosus*(pCXRR-lip); lane 3, *S. carnosus* Δ*tatAC*(pCX19); lane 4, *S. carnosus* Δ*tatAC*(pCXRR-lip). Plasmid pCX19 encodes lipase with a Sec SP, while pCXRR-lip encodes lipase with the Tat SP of FepB. The expression of lipase was induced by the addition of 0.5% xylose.

in kidneys were determined 5 days after infection. Our analysis revealed a significant lower virulence of the Δ*tatAC* mutant than that of the WT ($P = 0.041$). The median bacterial load in kidneys for the WT was 1.7×10^7 CFU, compared to 1.7×10^6 CFU for the Δ*tatAC* mutant. The difference between the WT and Δ*tat-fep* strains was less pronounced, but the bacterial load of the mutant was repeatedly lower than that of the WT (median, 1.7×10^7 versus 5.6×10^6 CFU) (Fig. 5B).

DISCUSSION

The twin-arginine translocation (Tat) pathway exists in many bacteria, archaea, and chloroplasts. In *S. aureus*, homologs of TatA and TatC have been identified. However, as mentioned in a recent review by Sibbald et al., the functionality of the *S. aureus* Tat translocase remains to be demonstrated (43). Yamada et al. compared a *tatC*-deficient mutant with its parent *S. aureus* strain by 2D gel electrophoresis and found no difference in the amounts of secreted staphylococcal enterotoxins and toxic shock syndrome toxin 1, whose SPs have some features often seen in signal sequences of Tat-dependent proteins, and they finally came to the conclusion that the Tat pathway does not play a major role in the secretion system of *S. aureus* (48). Here it is shown for the first time that the Tat pathway in *S. aureus* is functional and serves to translocate the iron-dependent peroxidase FepB.

In the genomes of various staphylococcal species, only one copy each of TatA and TatC could be identified; like the case in *Bacillus subtilis*, TatA seems to perform the functions of both the TatA and TatB components of *E. coli* (23). The TatA protein of staphylococci also contains both the phenylalanine residue (F20 in *E. coli* TatA) which is strictly conserved in the TatA/E proteins and the proline residue (P22 in *E. coli* TatB) which is strictly conserved in TatB proteins of gram-negative bacteria (see Fig. S1 in the supplemental material). Originally, our search in the *S. aureus* genome for potential Tat-dependent target proteins with a twin-arginine SP (RR-SP) motif revealed no promising candidates. However, in a search of the *S. carnosus* genome (36), the RR-SP in the iron-dependent peroxidase FepB was identified. As already mentioned, the RR-SP motif in the iron-dependent peroxidase (FepB) of *S. aureus* was wrongly annotated and therefore overlooked. Resequencing of the *S. aureus fepB* gene region indicated that the RR-SP motif was also present in *S. aureus* FepB.

Apart from FepB, no further protein with an RR-SP motif was discovered in the genome of *S. aureus* or *S. carnosus*, even though various search programs were used. Apparently, FepB is very likely the only Tat-dependent protein in staphylococci. As illustrated in Fig. 1A, FepB is encoded in an operon composed of a lipoprotein gene, *fepA*, the iron-dependent peroxidase gene, *fepB*, and a high-affinity iron transporter gene, *fepC*. In the opposite direction are the two TatA- and TatC-encoding genes. The *fep-tat* genes comprise not only a genetic but also a functional unit, since in the Δ*tatAC* mutants of *S. aureus* and *S. carnosus* the extracellular peroxidase activity is drastically decreased. To see whether other proteins were Tat dependent, we compared the secretomes of *S. carnosus* WT, *S. aureus* WT, and their Δ*tatAC* mutants by 2D gel electrophoresis; however, like Yamada et al. (48), we found no difference in the protein pattern, a further indication that FepB is the only Tat-dependent protein. However, the FepB spot could not be identified, as very likely it was masked by another protein spot. All results speak in favor of the hypothesis that the only function of the Tat system in *S. aureus* and also in *S. carnosus* is to translocate FepB. This was a bit surprising, as in many other gram-positive genera, such as *Bacillus*, *Streptomyces*, and *Mycobacterium*, many more proteins appear to be transported by the Tat system.

To our surprise, the analysis of the genomes of various staphylococcal species revealed that the *fep-tat* gene cluster is not present in all species. It is present in the genomes of all sequenced *S. aureus* strains as well as in *S. carnosus* and *S. haemolyticus*, but it is absent from the genomes of *S. epidermidis* and *S. saprophyticus*. By *tat*-specific PCR analysis, the list of staphylococcal species that possess or lack this gene cluster could be extended (see Results). It is conspicuous that the most aggressive human staphylococcal species, such as *S. aureus*, *S. haemolyticus*, and *S. lugdunensis*, possess the gene cluster, suggesting that it may contribute to aggravating an acute infection. Among those species that lack the gene cluster are *S. epidermidis* and *S. saprophyticus*, which are less aggressive and rather play a role in chronic infections. On the other hand, there are two apathogenic species representatives that also contain the *fep-tat* gene cluster. The natural habitat of *S. car-*

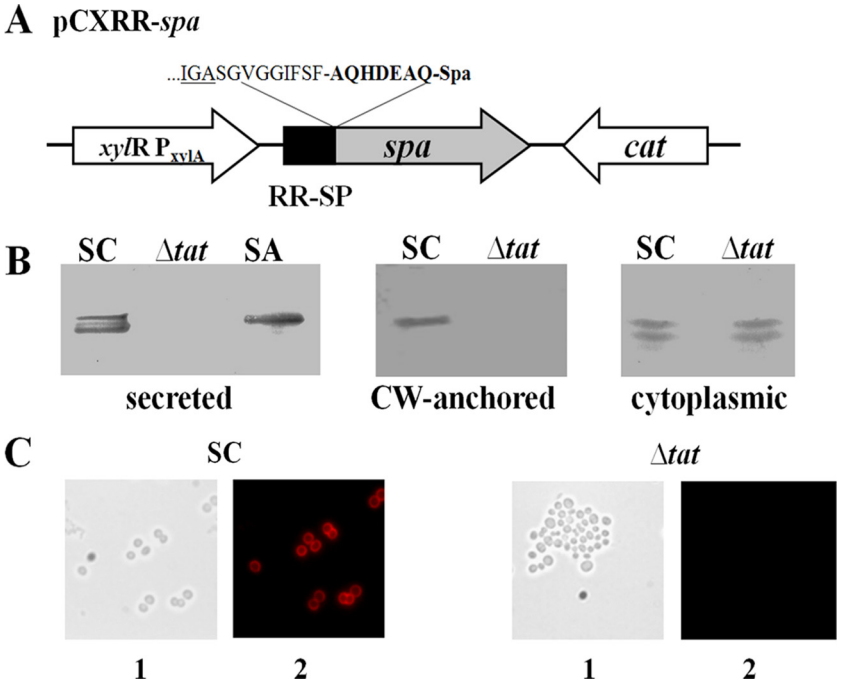

FIG. 4. Expression of pCXRR-spa. (A) Relevant part of plasmid pCXRR-spa encoding protein A under the control of a xylose-inducible promoter. Amino acids at the fusion site are indicated. (B) Western blot analysis of protein A expression in the culture supernatant, cell wall (CW)-anchored, and cytoplasmic fractions of *S. carnosus*(pCXRR-spa) and *S. carnosus* Δ*tatAC*(pCXRR-spa). *S. aureus* SA113 was used as a control. (C) Immunofluorescence labeling of protein A anchored to the cell wall, using Alexa Fluor 594-conjugated antibody. SC, *S. carnosus* WT. (1) Phase-contrast image. (2) Protein A visualized by immunofluorescence following antibody labeling.

nosus is meat (38), and that of S. *gallinarum* is the chicken crest (13). Presumably, in their particular environments, the iron-dependent peroxidase (FepB) is advantageous. The fact that the *fep-tat* gene cluster is not a common genus marker raises the question of its origin. Was it once a common part in the genome of the genus and got lost in those species where it was not needed, or was it acquired from other bacteria and kept in those staphylococcal species that benefitted most from the acquisition, such as the aggressive pathogens? There is some indication that at least in *S. aureus* and *S. carnosus* the *fep-tat* cluster might be a relic of a prophage, as immediately upstream of *tatA* there is a gene (SA0336 and SC2209, respectively) which encodes a protein with similarity to a phage envelope protein present in various staphylococcal phages but also in the phage of *Streptococcus mitis* SK137 (27). It might be possible that the *fep-tat* cluster in staphylococci has been spread by phages. On the other hand, in *S. haemolyticus* the *fep-tat* cluster is located differently and there is no phage-related gene nearby.

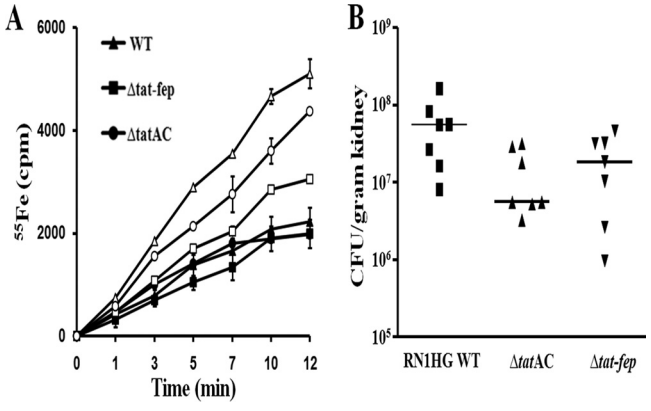

FIG. 5. (A) Iron transport. ^{55}Fe uptake was measured using cells grown under iron-sufficient (closed symbols) and iron-deficient (open symbols) conditions. The strains employed were *S. aureus* WT (△), *S. aureus* Δ*tatAC* (○), and *S. aureus* Δ*tat-fep* (□). Values presented are representative of three independent experiments. (B) Role of *S. aureus* RN1HG TatAC and FepABC in kidney infection. Bacterial loads of parental *S. aureus* and the *tatAC* and *tat-fep* mutant strains in the kidneys of BALB/c mice ($n = 7$) were determined 5 days after intravenous infection with 7×10^7 CFU. Each dot represents the bacterial load for one animal per gram of kidney.

The advantage of the *fep-tat* cluster could lie in iron uptake and in the external detoxification of H_2O_2, for example, in oxidative bursts during infection. Indeed, iron uptake under iron limitation was significantly decreased in the *fep-tat* mutants (Fig. 5A). The clear difference in iron uptake rates was surprising, as *S. aureus* has various Fe acquisition systems. However, there is only one inorganic Fe transporter (FeoAB), as the others are either siderophore dependent (such as SstABCD, SirABC, and FhuCBG) or transport heme-Fe (IsdDEF and HtsABC) (6). Our Fe transport assay suggests that the FepABC system transports inorganic Fe, with no indication that siderophores like staphyloferrins or aurochelin are involved. If the Fep system is also an inorganic Fe transporter, then its absence explains the observed clear decrease in the iron uptake rate.

To see whether the Fep-Tat system also has an effect in vivo, virulence studies with a mouse hematogenic kidney abscess

model were carried out with strain RN1HG, which is an *rsbU*-repaired 8325 strain and is more virulent than SA113 (Herbert et al., unpublished data). Therefore, the Δ*tatAC* and Δ*tat-fep* mutations were transduced into RN1HG. Indeed, it turned out that the bacterial load in the kidneys after 5 days was significantly lower for the Δ*tatAC* and Δ*tat-fep* mutants (Fig. 5B). The Δ*tatAC* mutant appeared even more attenuated than the Δ*tat-fep* mutant, which might be due to a fitness cost by accumulation of Fep protein in the cytoplasm. These results show that in the presence of the *fep-tat* cluster, fitness and virulence are increased during infection.

The functionality and specificity of the Tat system in both the *S. aureus* and *S. carnosus* backgrounds were also investigated, and it could be demonstrated that FepB is a Tat substrate that is recognized specifically by the Tat system. For the Δ*tatAC* mutants, the peroxidase activity was drastically decreased in the culture supernatant. The little residual activity seen in the mutants was probably due to some release of the cytoplasmic thioredoxin-dependent thiol peroxidase, which also breaks down H_2O_2 to water; a corresponding enzyme (SaurTPx) is at least annotated for various staphylococci. It has also been shown that the RR-SP is specific for the Tat system. Lipase fused with the FepB-derived RR-SP can be secreted only if the Tat system is functional, while secretion of lipase with its native SP was not affected in the Δ*tatAC* mutants. Most of these studies were carried out in the *S. carnosus* TM300 background, as this strain does not secrete active lipase or protein A that would interfere with monitoring (36). However, the results obtained with *S. carnosus* were frequently verified with *S. aureus* and its Δ*tatAC* mutant, which behaved quite similarly.

It is generally assumed that the Tat secretion system, in contrast to the Sec secretion system, translocates proteins that were completely folded and assembled in the cytoplasm. An interesting question was therefore whether proteins, such as protein A, that are covalently anchored by the sortase to the cell wall (28) can still be anchored when they are translocated by the Tat system. To address this question, the FepB-derived RR-SP was fused with protein A, and we compared its expression in TM300 and its Δ*tatAC* mutant. As illustrated in Fig. 4B, protein A could only be anchored in the WT, since the Δ*tatAC* mutant was unable to both translocate protein A to the medium and anchor it to the cell wall, although protein A was expressed in the cytoplasm of the Δ*tatAC* mutant. It is not known whether protein A is really completely folded during Tat-dependent translocation, but if it is folded it must be folded in such a way that the C-terminal sorting sequence is still accessible to the sortase to tether protein A to the cell wall. The cell wall-bound protein A was further demonstrated by immunofluorescence labeling (Fig. 4C).

The present study shows that the Tat pathway is functional in *S. aureus* and *S. carnosus* and that the iron-dependent peroxidase FepB is transported via this pathway. As indicated in Table 2, FepB homologues of other bacterial species from different phyla also have typical Tat signal sequences. Although peroxidase activity was detected in the supernatant of *S. carnosus* WT and no activity was detected for its Δ*tatAC* mutant, comparative 2D gel electrophoresis revealed no difference in the protein patterns. It may be that FepB is expressed only at low levels, such that its concentration is below the sensitivity limit of the current 2D gel electrophoresis technique.

Like the accessory Sec system, which exports exclusively one substrate, SraP (44), in *S. aureus*, the Tat system also appears to have only one substrate, FepB, or it could be that there are more Tat substrates which we failed to detect due to the sensitivity limitations of the techniques used. The most interesting finding was that the proteins routed through the Tat system can also be sortase substrates, and it would be interesting to know more about this mechanism. It would also be of interest to know why FepB should be transported via the Tat pathway.

ACKNOWLEDGMENTS

We thank Stefan Stevanovic (Institute for Cell Biology, University of Tübingen) for N-terminal sequencing of protein A and Regine Stemmler for technical assistance.

This work was supported by the DFG, graduate college GK685, the SFB766, and the BMBF PathoGenoMik (031U213B).

REFERENCES

1. **Bae, T., and O. Schneewind.** 2006. Allelic replacement in *Staphylococcus aureus* with inducible counter-selection. Plasmid **55:**58–63.
2. **Becker, K., D. Harmsen, A. Mellmann, C. Meier, P. Schumann, G. Peters, and C. von Eiff.** 2004. Development and evaluation of a quality-controlled ribosomal sequence database for 16S ribosomal DNA-based identification of *Staphylococcus* species. J. Clin. Microbiol. **42:**4988–4995.
3. **Berks, B. C., T. Palmer, and F. Sargent.** 2005. Protein targeting by the bacterial twin-arginine translocation (Tat) pathway. Curr. Opin. Microbiol. **8:**174–181.
4. **Berks, B. C., F. Sargent, and T. Palmer.** 2000. The Tat protein export pathway. Mol. Microbiol. **35:**260–274.
5. **Biswas, R., L. Voggu, U. K. Simon, P. Hentschel, G. Thumm, and F. Götz.** 2006. Activity of the major staphylococcal autolysin Atl. FEMS Microbiol. Lett. **259:**260–268.
6. **Brown, J. S., and D. W. Holden.** 2002. Iron acquisition by gram-positive bacterial pathogens. Microbes Infect. **4:**1149–1156.
7. **Brückner, R.** 1997. Gene replacement in *Staphylococcus carnosus* and *Staphylococcus xylosus*. FEMS Microbiol. Lett. **151:**1–8.
8. **Chaddock, A. M., A. Mant, I. Karnauchov, S. Brink, R. G. Herrmann, R. B. Klosgen, and C. Robinson.** 1995. A new type of signal peptide: central role of a twin-arginine motif in transfer signals for the delta pH-dependent thylakoidal protein translocase. EMBO J. **14:**2715–2722.
9. **Cid, H., M. Bunster, M. Canales, and F. Gazitua.** 1992. Hydrophobicity and structural classes in proteins. Protein Eng. **5:**373–375.
10. **De Buck, E., I. Lebeau, L. Maes, N. Geukens, E. Meyen, L. Van Mellaert, J. Anne, and E. Lammertyn.** 2004. A putative twin-arginine translocation pathway in Legionella pneumophila. Biochem. Biophys. Res. Commun. **317:**654–661.
11. **De Buck, E., L. Maes, E. Meyen, L. Van Mellaert, N. Geukens, J. Anne, and E. Lammertyn.** 2005. Legionella pneumophila Philadelphia-1 tatB and tatC affect intracellular replication and biofilm formation. Biochem. Biophys. Res. Commun. **331:**1413–1420.
12. **Devriese, L. A., V. Hájek, P. Oeding, S. A. Meyer, and K. H. Schleifer.** 1978. *Staphylococcus hyicus* (Sompolinsky 1953) comb. nov. and *Staphylococcus hyicus* subsp. *chromogenes* subsp. nov. Int. J. Syst. Bacteriol. **28:**482–490.
13. **Devriese, L. A., B. Poutrel, R. Kilpper-Bälz, and K. H. Schleifer.** 1983. *Staphylococcus gallinarum* and *Staphylococcus caprae*, two new species from animals. Int. J. Syst. Bacteriol. **33:**480–486.
14. **Dilks, K., R. W. Rose, E. Hartmann, and M. Pohlschroder.** 2003. Prokaryotic utilization of the twin-arginine translocation pathway: a genomic survey. J. Bacteriol. **185:**1478–1483.
15. **Freney, J., Y. Brun, M. Bes, H. Meugneir, F. Grimont, P. A. D. Grimont, C. Nervi, and J. Fleurette.** 1988. *Staphylococcus lugdunensis* sp. nov. and *Staphylococcus schleiferi* sp. nov., two species from human clinical specimens. Int. J. Syst. Bacteriol. **38:**168–172.
16. **Götz, F., T. Bannerman, and K. H. Schleifer.** 2006. The genera *Staphylococcus* and *Macrococcus*, p. 5–75. *In* M. Dworkin (ed.), Procaryotes, vol. 4. Springer, New York, NY.
17. **Götz, F., and K. H. Schleifer.** 1975. Purification and properties of a fructose-1,6-diphosphate activated L-lactate dehydrogenase from *Staphylococcus epidermidis*. Arch. Microbiol. **105:**303–312.
18. **Götz, F., H. M. Verheij, and R. Rosenstein.** 1998. Staphylococcal lipases: molecular characterisation, secretion, and processing. Chem. Phys. Lipids **93:**15–25.

19. **Guerout-Fleury, A. M., K. Shazand, N. Frandsen, and P. Stragier.** 1995. Antibiotic-resistance cassettes for *Bacillus subtilis*. Gene **167:**335–336.
20. **Hájek, V., W. Ludwig, K. H. Schleifer, N. Springer, W. Zitzelsberger, R. M. Kroppenstedt, and M. Kocur.** 1992. *Staphylococcus muscae*, a new species isolated from flies. Int. J. Syst. Bacteriol. **42:**97–101.
21. **Iordanescu, S., and M. Surdeanu.** 1976. Two restriction and modification systems in *Staphylococcus aureus* NCTC8325. J. Gen. Microbiol. **96:**277–281.
22. **Jongbloed, J. D., H. Antelmann, M. Hecker, R. Nijland, S. Bron, U. Airaksinen, F. Pries, W. J. Quax, J. M. van Dijl, and P. G. Braun.** 2002. Selective contribution of the twin-arginine translocation pathway to protein secretion in Bacillus subtilis. J. Biol. Chem. **277:**44068–44078.
23. **Jongbloed, J. D., U. Grieger, H. Antelmann, M. Hecker, R. Nijland, S. Bron, and J. M. van Dijl.** 2004. Two minimal Tat translocases in *Bacillus*. Mol. Microbiol. **54:**1319–1325.
24. **Kloos, W. E., and K. H. Schleifer.** 1975. Isolation and characterization of staphylococci from human skin. II. Description of four new species: *Staphylococcus warneri*, *Staphylococcus capitis*, *Staphylococcus hominis*, and *Staphylococcus simulans*. Int. J. Syst. Bacteriol. **25:**62–79.
25. **Kuroda, M., T. Ohta, I. Uchiyama, T. Baba, H. Yuzawa, I. Kobayashi, L. Cui, A. Oguchi, K. Aoki, Y. Nagai, J. Lian, T. Ito, M. Kanamori, H. Matsumaru, A. Maruyama, H. Murakami, A. Hosoyama, Y. Mizutani-Ui, N. K. Takahashi, T. Sawano, R. Inoue, C. Kaito, K. Sekimizu, H. Hirakawa, S. Kuhara, S. Goto, J. Yabuzaki, M. Kanehisa, A. Yamashita, K. Oshima, K. Furuya, C. Yoshino, T. Shiba, M. Hattori, N. Ogasawara, H. Hayashi, and K. Hiramatsu.** 2001. Whole genome sequencing of meticillin-resistant *Staphylococcus aureus*. Lancet **357:**1225–1240.
26. **Liebl, W., and F. Götz.** 1986. Studies on lipase directed export of *Escherichia coli* beta-lactamase in *Staphylococcus carnosus*. Mol. Gen. Genet. **204:**166–173.
27. **Llull, D., R. Lopez, and E. Garcia.** 2006. Skl, a novel choline-binding N-acetylmuramoyl-L-alanine amidase of *Streptococcus mitis* SK137 containing a CHAP domain. FEBS Lett. **580:**1959–1964.
28. **Mazmanian, S. K., H. Ton-That, and O. Schneewind.** 2001. Sortase-catalysed anchoring of surface proteins to the cell wall of *Staphylococcus aureus*. Mol. Microbiol. **40:**1049–1057.
29. **McDonough, J. A., K. E. Hacker, A. R. Flores, M. S. Pavelka, Jr., and M. Braunstein.** 2005. The twin-arginine translocation pathway of *Mycobacterium smegmatis* is functional and required for the export of mycobacterial beta-lactamases. J. Bacteriol. **187:**7667–7679.
30. **Meissner, D., A. Vollstedt, J. M. van Dijl, and R. Freudl.** 2007. Comparative analysis of twin-arginine (Tat)-dependent protein secretion of a heterologous model protein (GFP) in three different gram-positive bacteria. Appl. Microbiol. Biotechnol. **76:**633–642.
31. **Ochsner, U. A., A. Snyder, A. I. Vasil, and M. L. Vasil.** 2002. Effects of the twin-arginine translocase on secretion of virulence factors, stress response, and pathogenesis. Proc. Natl. Acad. Sci. USA **99:**8312–8317.
32. **Ollinger, J., K. B. Song, H. Antelmann, M. Hecker, and J. D. Helmann.** 2006. Role of the Fur regulon in iron transport in *Bacillus subtilis*. J. Bacteriol. **188:**3664–3673.
33. **Peschel, A., B. Ottenwälder, and F. Götz.** 1996. Inducible production and cellular location of the epidermin biosynthetic enzyme EpiB using an improved staphylococcal expression system. FEMS Microbiol. Lett. **137:**279–284.
34. **Resch, A., S. Leicht, M. Saric, L. Pasztor, A. Jakob, F. Gotz, and A. Nordheim.** 2006. Comparative proteome analysis of *Staphylococcus aureus* biofilm and planktonic cells and correlation with transcriptome profiling. Proteomics **6:**1867–1877.
35. **Robinson, C., and A. Bolhuis.** 2004. Tat-dependent protein targeting in prokaryotes and chloroplasts. Biochim. Biophys. Acta **1694:**135–147.
36. **Rosenstein, R., C. Nerz, L. Biswas, A. Resch, G. Raddatz, S. C. Schuster, and F. Götz.** 2009. Genome analysis of the meat starter culture bacterium *Staphylococcus carnosus* TM300. Appl. Environ. Microbiol. **75:**811–822.
37. **Santini, C. L., B. Ize, A. Chanal, M. Muller, G. Giordano, and L. F. Wu.** 1998. A novel sec-independent periplasmic protein translocation pathway in Escherichia coli. EMBO J. **17:**101–112.
38. **Schleifer, K. H., and U. Fischer.** 1982. Description of a new species of the genus *Staphylococcus*: *Staphylococcus carnosus*. Int. J. Syst. Bacteriol. **32:**153–156.
39. **Schleifer, K. H., and W. E. Kloos.** 1975. Isolation and characterization of staphylococci from human skin. I. Amended descriptions of *Staphylococcus saprophyticus* and descriptions of three new species: *Staphylococcus cohnii*, *Staphylococcus haemolyticus*, and *Staphylococcus xylosus*. Int. J. Syst. Bacteriol. **25:**50–61.
40. **Schmollinger, M., I. Fischer, C. Nerz, S. Pinkenburg, F. Gotz, M. Kaufmann, K. J. Lange, R. Reuter, W. Rosenstiel, and A. Zell.** 2004. ParSeq: searching motifs with structural and biochemical properties. Bioinformatics **20:**1459–1461.
41. **Schneewind, O., P. Model, and V. A. Fischetti.** 1992. Sorting of protein A to the staphylococcal cell wall. Cell **70:**267–281.
42. **Severance, S., S. Chakraborty, and D. J. Kosman.** 2004. The Ftr1p iron permease in the yeast plasma membrane: orientation, topology and structure-function relationships. Biochem. J. **380:**487–496.
43. **Sibbald, M. J., A. K. Ziebandt, S. Engelmann, M. Hecker, A. de Jong, H. J. Harmsen, G. C. Raangs, I. Stokroos, J. P. Arends, J. Y. Dubois, and J. M. van Dijl.** 2006. Mapping the pathways to staphylococcal pathogenesis by comparative secretomics. Microbiol. Mol. Biol. Rev. **70:**755–788.
44. **Siboo, I. R., D. O. Chaffin, C. E. Rubens, and P. M. Sullam.** 2008. Characterization of the accessory Sec system of *Staphylococcus aureus*. J. Bacteriol. **190:**6188–6196.
45. **Strauss, A., and F. Götz.** 1996. In vivo immobilization of enzymatically active polypeptides on the cell surface of *Staphylococcus carnosus*. Mol. Microbiol. **21:**491–500.
46. **Takeuchi, F., S. Watanabe, T. Baba, H. Yuzawa, T. Ito, Y. Morimoto, M. Kuroda, L. Cui, M. Takahashi, A. Ankai, S. Baba, S. Fukui, J. C. Lee, and K. Hiramatsu.** 2005. Whole-genome sequencing of *Staphylococcus haemolyticus* uncovers the extreme plasticity of its genome and the evolution of human-colonizing staphylococcal species. J. Bacteriol. **187:**7292–7308.
47. **Wieland, K. P., B. Wieland, and F. Gotz.** 1995. A promoter-screening plasmid and xylose-inducible, glucose-repressible expression vectors for *Staphylococcus carnosus*. Gene **158:**91–96.
48. **Yamada, K., I. Sanzen, T. Ohkura, A. Okamoto, K. Torii, T. Hasegawa, and M. Ohta.** 2007. Analysis of twin-arginine translocation pathway homologue in *Staphylococcus aureus*. Curr. Microbiol. **55:**14–19.